ADVANCED FUNCTIONAL MATERIALS

FULL PAPER

# Photochemically Controlled Photonic Crystals**

By *Marta Kamenjicki*, *Igor K. Lednev*, *Alexander Mikhonin*, *Rasu Kesavamoorthy*, and *Sanford A. Asher**

We have developed photochemically controlled photonic crystals that may be useful in novel recordable and erasable memories and/or display devices. These materials can operate in the UV, visible, or near-IR spectral regions. Information is recorded and erased by exciting the photonic crystal with ~360 nm UV light or ~480 nm visible light. The information recorded is read out by measuring the photonic crystal diffraction wavelength. The active element of the device is an azobenzene-functionalized hydrogel, which contains an embedded crystalline colloidal array. UV excitation forms *cis*-azobenzene while visible excitation forms *trans*-azobenzene. The more favorable free energy of mixing of *cis*-azobenzene causes the hydrogel to swell and to red-shift the photonic crystal diffraction. We also observe fast nanosecond, microsecond, and millisecond transient dynamics associated with fast heating lattice constant changes, refractive index changes, and thermal relaxations.

## 1. Introduction

The recent intense interest in photonic bandgap crystals stems from their potential ability to increase light waveguiding efficiency, to increase the efficiency of stimulated emission processes, and to localize light.[1] Numerous groups around the world are developing fabrication methods to produce photonic crystals with bandgaps in the visible, infrared, and microwave spectral regions.[2]

The simplest photonic crystal can be fabricated by the close-packing of spheres, similar to that which in nature forms opals.[3] The earliest chemical approach fabricated large face-centered cubic (fcc) photonic bandgap crystals through the self-assembly of highly charged, monodisperse colloidal particles into crystalline colloidal arrays (CCAs). The CCAs self-assemble due to long-range electrostatic repulsions between particles.[4]

These CCAs are complex fluids which consist of colloidal particles which self-assemble into plastic fcc crystalline arrays that Bragg-diffract ultraviolet, visible, or near-infrared light, depending on the colloidal particle array spacings. More recently, robust semi-solid photonic crystal (PCCA) materials were fabricated by polymerizing a hydrogel network around the self-assembled CCA array[5] (Fig. 1). This new photonic crystal material can utilize environmentally responsive hydrogels[6] to create a PCCA in which thermal or chemical environmental alterations result in PCCA volume change, thereby altering the CCA photonic crystal plane spacings and diffraction wavelengths.[7–11]

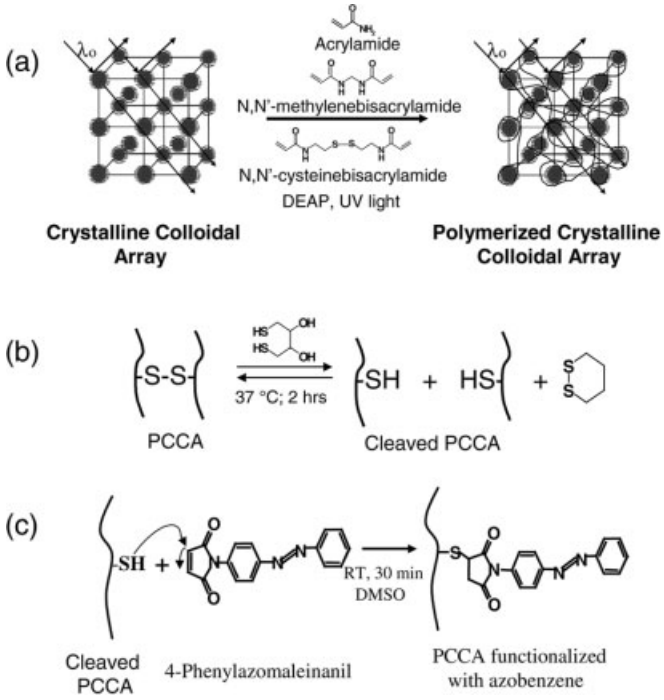


Fig. 1. a) Synthesis of the PCCA-containing disulfide bonds. b) Cleaving disulfide bonds with DTT. c) Maleimide-thiol attachment of azobenzene to PCCA.

We report here the development of a photochemically actuated PCCA (120 nm diameter polystyrene CCA), where photoisomerization of a covalently attached chromophore changes the hydrogel free energy of mixing. The resulting photocontrolled PCCA (PCPCCA) volume change alters the lattice constant and shifts the diffracted wavelength. Thus, we have a material in which we modulate the diffracted light by the independent absorption of light outside the diffraction bandgap.

[*] Prof. S. A. Asher, M. Kamenjicki, A. Mikhonin
Department of Chemistry, University of Pittsburgh
Pittsburgh, PA 15260 (USA)
E-mail: asher@pitt.edu
Dr. I. K. Lednev
Department of Chemistry, University at Albany, SUNY
Albany, NY 12222 (USA)
Dr. R. Kesavamoorthy
Materials Science Division, Indira Gandhi Centre for Atomic Research
Kalpakkam 603 102 (India)

[**] We gratefully acknowledge financial support from ONR, NSF, and DARPA.

  **DOI:** 10.1002/adfm.200304424 *Adv. Funct. Mater.* **2003**, *13*, No. 10, October

ADVANCED FUNCTIONAL MATERIALS



## 2. Results and Discussion

### 2.1. Photochemistry of 4-Phenylazomaleinanil Solution

Azobenzene derivatives, which are normally in their ground state trans forms at room temperature in the dark,[12–17] show strong $\pi \rightarrow \pi^*$ absorption bands at ~340 nm (Fig. 2). 4-phenylazomaleinanil shows the typical azobenzene photochemistry,

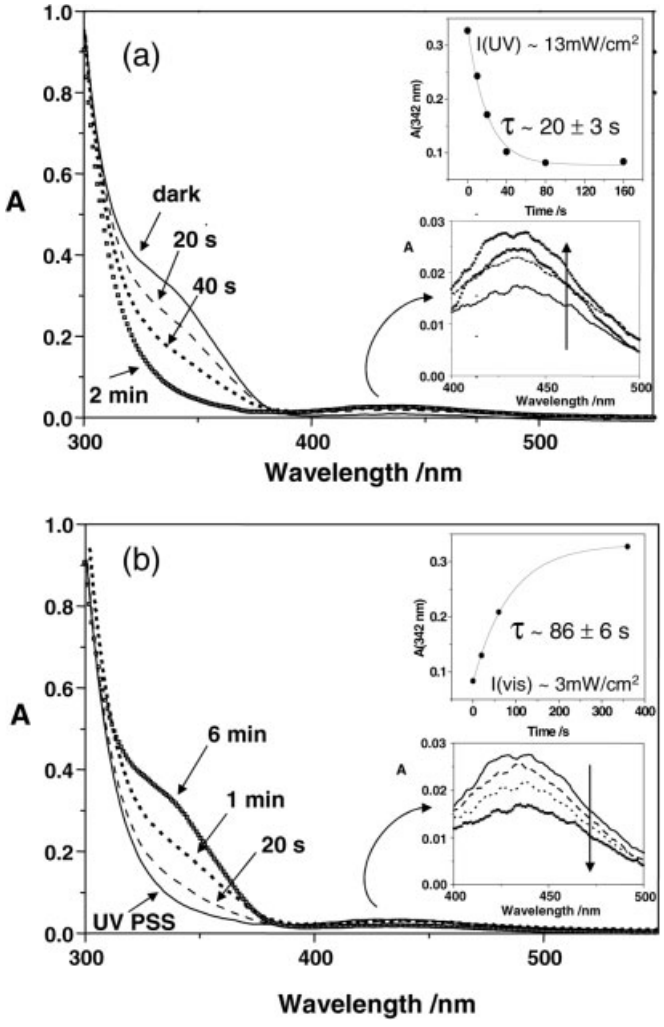


Fig. 2. Photochemistry of 60 μM 4-phenylazomaleinanil in DMSO in a 1 mm quartz cuvette. a) Absorption changes upon irradiation with 13 mW cm$^{-2}$ of 365 nm light. b) Absorption changes upon irradiation with 3 mW cm$^{-2}$ of white light. The UV PSS curve shows the photostationary state absorption reached with UV light excitation.

where irradiation with 365 nm UV light bleaches the strong ~340 nm trans $\pi \rightarrow \pi^*$ UV absorption band as it converts *trans*-azobenzene to the cis form. A weaker cis $n \rightarrow \pi^*$ absorption band at ~435 nm (Fig. 2a) appears. Figure 2a shows that irradiation of a dimethylsulfoxide (DMSO) solution of 4-phenylazomaleinanil by ~13 mW cm$^{-2}$ of 365 nm UV light from a mercury lamp gives rise to a photostationary state within 2 min. This is expected from the ~20 s observed bleaching time of the ~340 nm trans band of the 4-phenylazomaleinanil DMSO solution (Fig. 2a, inset). Subsequent irradiation with white light (~3 mW cm$^{-2}$, from a fiber-optic-coupled tungsten lamp with a UV rejection filter) photoconverts the cis form back to the trans form, as shown by the restored ~340 nm trans $\pi \rightarrow \pi^*$ absorption (Fig. 2b).The Figure 2b inset indicates a ~86 s characteristic time for photoisomerization back to the trans form.

We have roughly determined that the trans to cis quantum yield is $\Phi \approx 0.07$ for our 4-phenylazomaleinanil in iso octane for 355 nm excitation. This quantum yield is comparable to that of azobenzene in iso octane ($\Phi \approx 0.12$).[18–22] In addition, we observe that 4-phenylazomaleinanil dissolved in DMSO (4.5 mM) shows very similar kinetics to 4.5 mM 4-phenylazomaleinanil attached to a PCCA, which also indicates similar quantum yields.

### 2.2. Photophysics of PCCA Functionalized with Azobenzene

Figure 3 shows the absorption spectrum of a PCCA containing covalently attached azobenzene (PCPCCA). The PCPCCA photochemistry observed is essentially identical to that of

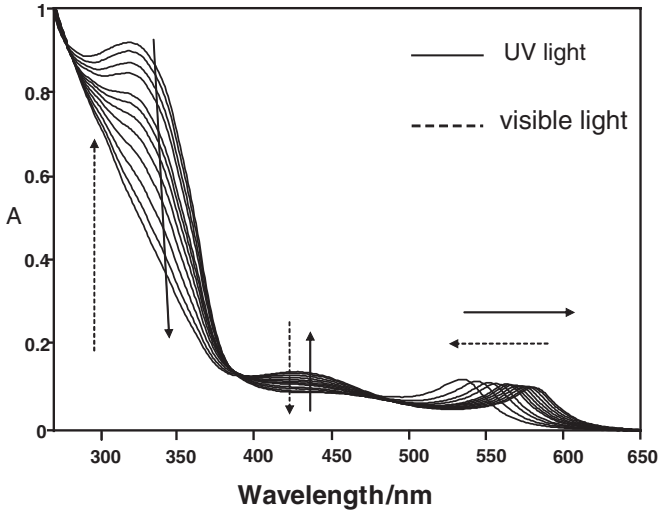


Fig. 3. 40 μm thick PCCA functionalized with 4-phenylazomaleinanil (3 mM) shows a 50 nm diffraction red shift upon UV excitation. Solid arrows show spectral changes due to the UV irradiation, while the dashed arrows show changes due to visible light illumination. The 530–600 nm peak derives from diffraction by the PCCA fcc (111) planes. The (111) plane spacing, $d_{111} = \lambda_0/2n$ for light at normal incidence.

4-phenylazomaleinanil in DMSO. Excitation with 365 nm UV light (~13 mW cm$^{-2}$) results in a decrease in the 322 nm ($\pi \rightarrow \pi^*$) trans absorption and an increase in the 430 nm ($n \rightarrow \pi^*$) cis absorption, due to the photoconversion of the trans to the cis form (the absorption shifts to 322 nm upon attachment to the PCCA).

The PCCA was oriented such that the beam was incident normal to the fcc (111) planes, which at this normal incidence diffracts ~530 nm light. The conversion of *trans*-azobenzene to the cis form causes the (111) plane diffraction to shift from ~530 nm to ~580 nm. Excitation with visible light (~3 mW cm$^{-2}$) shifts the diffraction back to ~530 nm.

  

The diffraction red shift is due to an increase in the free energy of mixing of the hydrogel polymer network with the medium upon UV light illumination, while the blue shift results from a decrease in the free energy of mixing upon return of the azobenzene to its trans form.

This photochemically driven diffraction change is reversible as shown in Figure 4, which shows a sample cycled numerous times by UV and visible excitation. Irradiation of a cycled

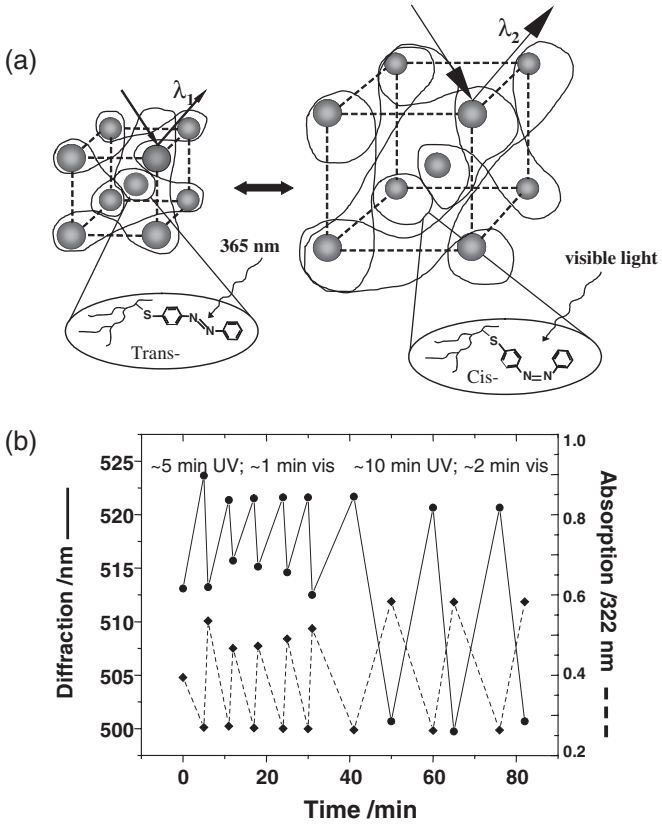


Fig. 4. a) UV light photoisomerizes the trans to the cis derivative, while visible light photoisomerizes the cis to the trans form. b) Reversible photochemistry: UV light red shifts the diffraction and bleaches the trans 322 nm absorption, while subsequent excitation with visible light blue shifts the diffraction and increases the 322 nm absorption.

PCPCCA (where the fcc (111) plane diffracts at ~513 nm) for 5 min with ~10 mW cm$^{-2}$ UV light causes a ~0.2 absorbance decrease at ~322 nm and a ~5 nm diffraction red shift, which is completely reversed by 1 min illumination with ~50 mW cm$^{-2}$ visible light. Doubling the visible illumination time increases the 322 nm trans absorption and causes the diffraction shift to double. The ~520 nm maximum diffraction value occurs in a sample that was converted to the cis form and which shows a maximum trans photobleach. Doubling the visible wavelength excitation duration essentially doubles the conversion to the trans derivative, which doubles the blue shift. We are surprised that we do not observe a doubling of the 322 nm trans absorption. The PCPCCA absorption and diffraction can be cycled back and forth indefinitely.

Thermal cis → trans relaxation in the dark gradually blue shifts the diffraction (Fig. 5a) as the azobenzene relaxes to its

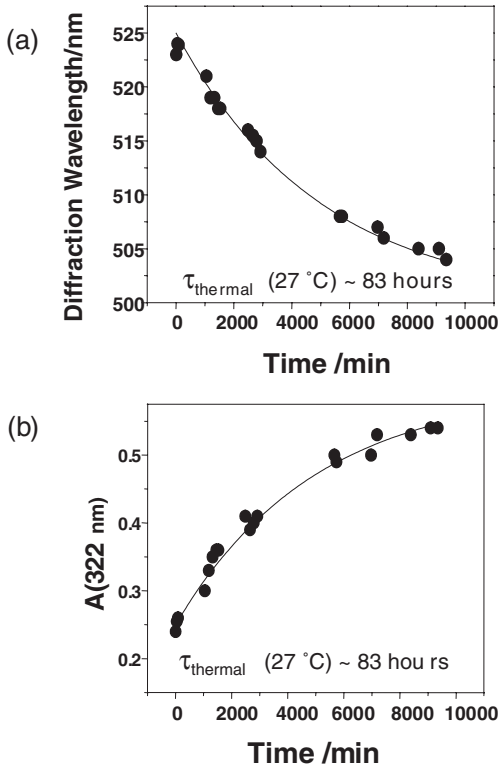


Fig. 5. Thermal isomerization of azobenzene attached to a PCCA at 27 °C in the dark. a) Diffraction wavelength and b) 322 nm absorption changes.

thermodynamically more stable trans state, which restores the 322 nm trans absorption (Fig. 5b). This dark relaxation is very slow (~83 h at 27 °C) compared to the observed photoisomerization rates.

In our study we determined the activation energy for the ground state cis–trans isomerization by measuring the thermal relaxation for the cis–trans process in dark at different temperatures. Characteristic times were determined for seven different temperatures, from which we calculate an activation energy of 28 kcal mol$^{-1}$ for the ground-state cis–trans isomerization of the 4-phenylazomaleinanil functionalized PCCA (Table 1).

Table 1. Temperature dependence of the PCPCCA dark thermal relaxation.

| Temperature [°C] | *t* [h] |
|---|---|
| 27 | 83 |
| 28 | 64 |
| 35 | 28 |
| 36 | 23 |
| 42 | 13 |
| 49 | 3 |
| 56 | 1.4 |

The magnitude of the diffraction shift photoresponse increases monotonically with increasing azobenzene concentration (Fig. 6) due to the resulting increased free energy of mixing change. As expected, the photoresponse decreases as the hydrogel cross-linking density increases, due to the resulting increased elastic constants of the PCCA. No photoresponse

  

ADVANCED FUNCTIONAL MATERIALS



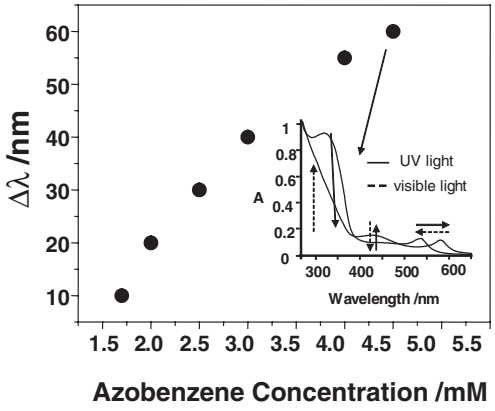


Fig. 6. Dependence of photoresponse on 4-phenylazomaleinanil concentration (in DMSO medium). Inset shows the absorption spectrum of a PCPCCA containing 4.5 mM of 4-phenylazomaleinanil.

occurs for > 10 % concentrations of *N,N′*-methylenebisacrylamide relative to acrylamide (Fig. 7). The cross-link concentrations displayed are those expected for the stoichiometric incorporation of *N,N′*-methylenebisacrylamide as PCCA cross-links,

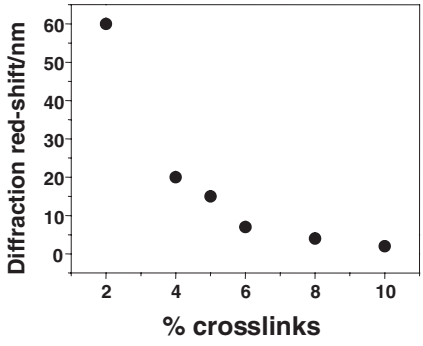


Fig. 7. Dependence of diffraction shift on the cross-link concentration (bisacrylamide relative to acrylamide). We expect a much smaller actual cross-link density [11]. The gel thickness is 80 μm and contains 4.5 mM azobenzene.

assuming that all of the *N,N′*-cystaminebisacrylamide disulfide bonds were broken. However, it should be noted that the effective cross-link concentration is usually found to be significantly below this stoichiometric concentration; Asher and co-workers[8] demonstrated that only a small fraction of the *N,N′*-methylenebiscrylamide cross-linker forms effective hydrogel cross-links.

### 2.3. Diffraction Kinetics

The response time of the PCPCCA diffraction shift can be limited by the actinic power, the photolysis rates, and by the collective diffusion constant of the hydrogel polymer network. Our diffraction shifts can be actuated by a single nanosecond laser pulse. Figure 8a shows that a single 0.4 mJ cm$^{-2}$, 3 ns, 355 nm pulse from a yttrium aluminum garnet (YAG) laser actuates a trans bleach and causes a ~7 nm diffraction red shift for a PCPCCA that normally diffracts at ~440 nm. The response of the sample is additive; three 355 nm pulses cause ~3 times the red shift (Fig. 8a). As shown in Figure 8b we can

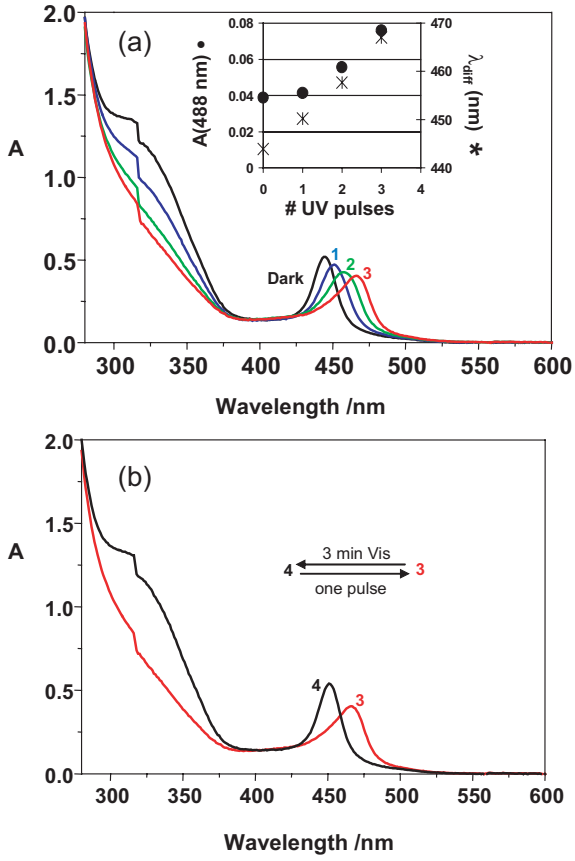


Fig. 8. a) Extinction changes induced in PCPCCA by three laser pulses (355 nm, 0.4 J cm$^{-2}$). b) System returns back to the original state after 3 min of ~50 mJ cm$^{-2}$ visible irradiation (3 to 4). One 1.2 J cm$^{-2}$ 355 nm laser pulse induces a 20 nm diffraction red shift (4 to 3).

achieve the same red shift with one 1.2 mJ cm$^{-2}$ pulse. The response can be erased with visible light, and it is completely reversible over an indefinite number of cycles.

We examined the kinetics of the diffraction changes by monitoring changes in the transmission spectrum of the sample after applying one 355 nm YAG pulse (1.2 mJ cm$^{-2}$, 3 ns duration). We used a 120 ns pulsed Xe flashlamp (IBH Model 5000XeF) and Ocean Optics USB2000 Miniature Fiber Optic Spectrometer (Fig. 9) and recorded spectra after time delays of 0.3 μs to 6 ms,

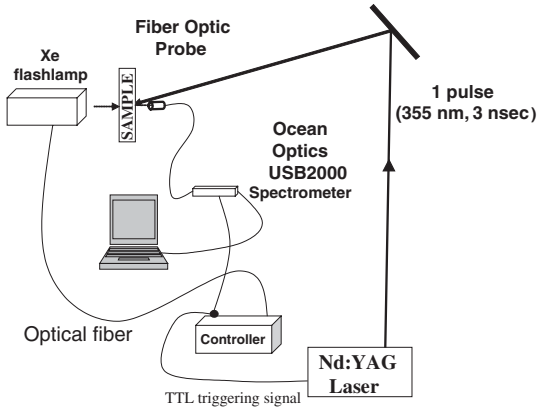


Fig. 9. Transient absorption spectrophotometer used to measure PCPCCA spectral kinetic responses to 355 nm light.

  

and 3 s to 2 min after UV pulses. As an example, Figure 10a shows spectra recorded before (black) and at various times (0.3–6000 μs) after excitation (red) by a 3 ns 355 nm pulse. The final state of the sample was recorded 1 min after this UV pulse (blue). In addition, Figure 11 graphically shows the time dependence of diffraction maximum wavelength on the slow second timescale.

A diffraction red shift of ~5 nm occurs within 300 ns. The diffraction peak remains sharp and symmetric. At 1.3 μs we see more complex dynamics where the background increases and the diffraction broadens. The diffraction continues to red shift until ~12 μs. By 100 μs the diffraction begins to narrow and the diffraction band blue shifts. At 302 μs only a small diffraction red shift remains; the diffraction spectrum is close to that prior to the UV pulse.

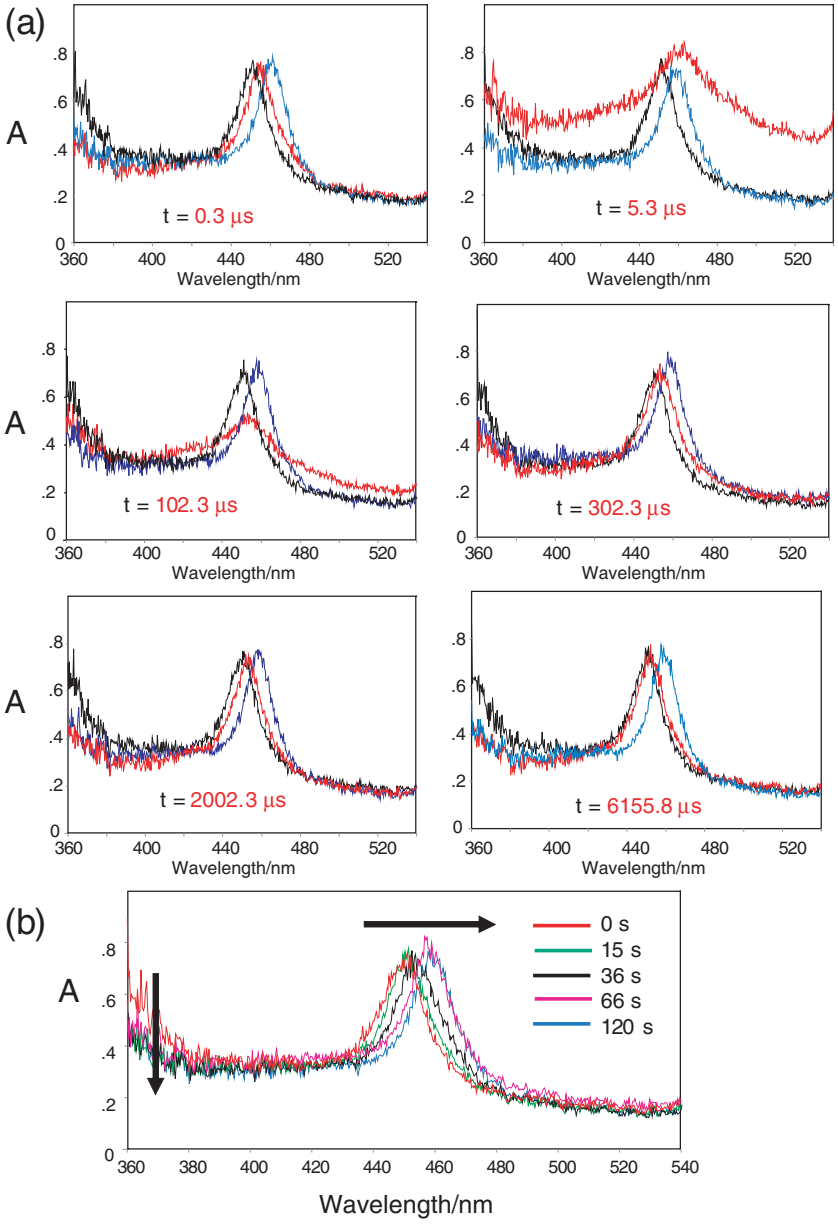


Fig. 10. a) PCPCCA in dark (black), at the indicated time subsequent to excitation by one 3 ns 355 nm pulse (red), and after 1 min (blue). b) Absorption spectral changes in second time regime.

Much larger diffraction changes (~10 nm) occur at much longer times (~20 s, Figs. 10b,11). The fact that the 365 nm absorption remains bleached demonstrates that this slow process does not involve azobenzene trans-to-cis ground-state photochemistry. This slow time scale is typically observed[9] for macroscopic volume phase transitions of 2 cm × 2 cm × 80 μm photonic crystals in response to changes in the free energy of mixing or changes in the Donnan potential. This process is delayed by the polymer collective diffusion constant and by the necessity of mass flow in order for the DMSO solvent outside the hydrogel to flow into the swelling polymer.[23] Thus, this slow diffraction shift results from a hydrogel volume phase transition driven by the change in the free energy of mixing of *cis*-azobenzene compared to *trans*-azobenzene.

Clearly, other dynamic phenomena come into play in the shorter time regimes. The prompt (0.3 μs) ~4 nm rigid diffraction band red shift, which preserves the diffraction peak shape, appears to directly result from heating of the PCCA by the incident UV beam. The PCCA, which is rigidly attached to a quartz surface, is composed mainly of DMSO, which shows a temperature-dependent density around room temperature of $d\rho/dT = -0.0012$.[24] We calculate that our UV pulse beam essentially instantly induces a 20 °C temperature jump in the sample that expands the PCCA volume, thereby increasing $d_{111}$ to red shift the diffraction. A counteracting diffracted wavelength blue shift must also accompany the resulting temperature-induced refractive index decrease ($dn/dT = -0.00035$ for DMSO).[24]

In general, we find that the total volume change of a hydrogel is determined by its thermodynamics. The exact diffraction change depends upon whether the hydrogel expansion is constrained. If the hydrogel is unconstrained the linear dimensional change in any direction $d'_{111}/d_{111} = (V'/V)^{1/3}$. In contrast, for hydrogels attached to a quartz surface, the entire volume change can only occur along the normal to the surface. Thus, $d'_{111}/d_{111} = V'/V$. In this case the 20 °C temperature rise would increase the volume by ~2 % which would increase $d_{111}$ and the wavelength diffracted by a maximum of 9 nm. In contrast, the 0.007 decrease in $n$ would decrease the diffracted wavelength by 3 nm. The resultant 6 nm estimated shift is very close to the 5 nm shift observed.

This hypothesis of heating as being responsible for this prompt diffraction shift is supported by observations of prompt *T*-jump diffraction red shifts for samples where azobenzene is dissolved in the hydrogel at identical concentrations rather than being at-

ADVANCED FUNCTIONAL MATERIALS



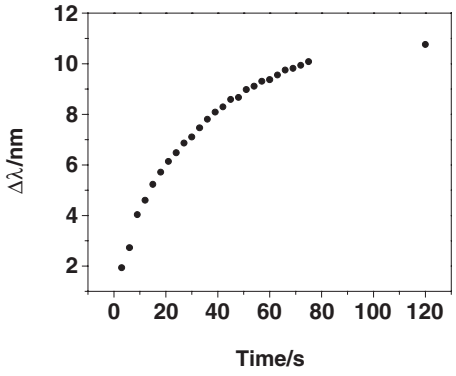


Fig. 11. Temporal dependence of diffraction peak wavelength after excitation by a 3 ns 355 nm laser pulse.

tached, and by our observations that the magnitude of the red shift scales with pulse energy.

The scattering baseline increases and the diffraction band broadens during 5–100 μs after the UV pulse. These phenomena must result from transient disordering within the PCCA. Although our mesoscopically inhomogeneous material inhomogeneously absorbs the UV light to give rise to an instantaneous mesoscopic inhomogeneous temperature redistribution, the temperature should become uniformly distributed well within 50 ns.[25]

The ~50 μs disorder dynamics must originate from longer scale phenomena in the sample. The PCCA can be thought of as 120 nm slabs containing colloidal particles arrayed within a hydrogel containing DMSO, separated by ~30 nm slabs of a hydrogel containing DMSO. We excite an internal 2 mm × 2 mm × 80 μm volume element of the PCCA by a UV pulse. This heated volume element must then expand against the adjacent, cooler hydrogel. This results in lateral constraining forces. These compressive restoring forces create an instability in the heated hydrogel.

It is well known that smectic liquid crystals (which have analogous structures) respond to such constraints by having their layers buckle and at high strains forming parabolic focal conics.[26,27] Analogous forces in our case will cause the (111) layers to buckle, which will cause the (111) planes to show a distribution of shallow tilt angles relative to the excitation beam. This causes the diffraction band to broaden. Other defect structures that form will cause additional light scattering.

This constraint decreases as the probed volume thermally reequilibrates on the ~200 μs timescale that restores the original diffraction peak after 6 ms. In the multisecond time domain, the system undergoes a free energy of mixing change volume phase transition driven by the trans–cis photoisomerization of the azobenzene.

This PCPCCA functions as a slow display device, and may be used as a novel recordable and erasable memory material. Light absorption actuates the diffraction shift. This diffraction shift is read out at a wavelength where no absorption occurs. Our photonic crystal material can be addressed and read out in small areas. For example, we should be able to utilize pixels as small as ~1 μm, the smallest region which can give rise to a narrow diffraction band. Reading this device is limited only by the speed with which the material can be scanned or imaged by a laser beam.

## 3. Conclusions

Diffraction switching in our PCPCCA results from both azobenzene photoisomerization and laser heating. In the fast nanosecond time regime, heating increases the material volume and red shifts the diffraction. This volume change relaxes in the microsecond time domain. At longer times the volume of the PCPCCA hydrogel is controlled by the balance between the free energy of mixing of the polymer hydrogel with DMSO and the elastic restoring force of the hydrogel cross-links. The higher *cis*-isomer dipole moment results in an increased solubility in DMSO, causing an increase in the free energy of mixing. Thus the PCPCCA swells and a diffraction red shift is observed. To our knowledge, this is the first example of the photochemical control of a photonic crystal.

## 4. Experimental

The highly sulfonated, 120 nm diameter monodisperse colloidal particles were prepared by emulsion polymerization [28]. After dialyzing against water for one week these particles readily self-assemble into highly ordered CCAs. *N,N′*-cystaminebisacrylamide (5 mg; Aldrich) dissolved in 20 μL DMSO was added to 4 mg of a solution of 10 % diethoxyacetophenone (DEAP, Aldrich, v/v) in DMSO. The PCCA were prepared by adding this solution to a solution containing 50 mg acrylamide (Sigma), 3 mg *N,N′*-methylenebisacrylamide (Sigma), and 1 g of a 10 wt.-% dispersion of diffracting polystyrene CCAs (Fig. 1a). This solution was injected into a cell made of two quartz plates separated by a 80 μm thick spacer and exposed to UV light (Black-Ray model B-100A, UVP Inc.). After 30 min illumination, the cell was opened and the gel was removed and washed with water. The PCCA remained attached to one of the quartz plates.

Dithiolthreitol (DTT, ACROS Organics) was used to cleave the PCCA disulfide bonds (Fig. 1b), which leaves reactive thiol groups attached to the PCCA [29,30]. The PCCA diffraction red shifts upon cleavage of these disulfide bond cross-links, due to the resulting decrease in the PCCA elastic constant.

The medium within the cleaved PCCA was slowly exchanged with pure DMSO; the PCCA diffraction efficiency decreased due to the smaller refractive index difference between the polystyrene colloids ($n = 1.6$) and the DMSO ($n = 1.47$) containing medium, compared to that of water ($n = 1.33$). The PCCA volume decreased somewhat, due to the decrease in the free energy of mixing between the PCCA and DMSO, compared to water.

The PCCA was incubated under stirring for ~2 h with a solution of 4-phenylazomaleinanil (Polysciences, Inc) (Fig. 1c) in DMSO (7 mM). Figure 12 compares

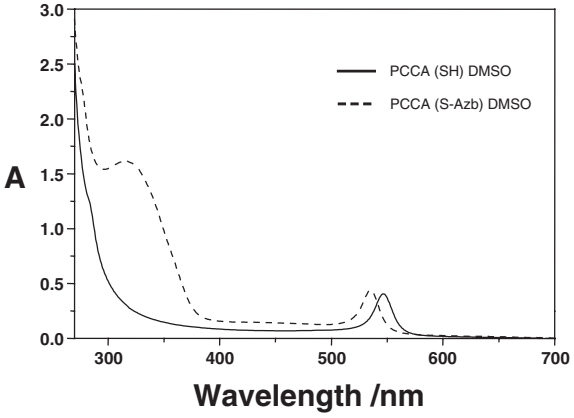


Fig. 12. Absorption spectra of 80 μm thick PCCA before and after attachment of a 4-phenylazomaleinanil.

  

the absorption spectrum of the PCCA before and after attachment of the azobenzene derivative. In the absence of azobenzene the PCCA shows diffraction from the fcc (111) planes at ~540 nm. Below 300 nm, the spectrum also shows contributions from higher order diffraction, as well as from the polystyrene colloid particle absorption.

In contrast, the PCCA containing covalently attached azobenzene additionally shows the trans azobenzene 322 nm absorption band. We can vary the amount of attached azobenzene by controlling the sulfhydryl group concentration within the PCCA.

Received: May 27, 2003
Final version: June 19, 2003

[1] J. D. Joannopoulos, R. D. Meade, J. N. Winn, *Photonic Crystals: Molding the Flow of Light*, Princeton University Press, New York **1995**.
[2] a) T. F. Krauss, R. M. De La Rue, *Prog. Quantum Electron.* **1999**, *23*, 51. b) G. A. Azin, S. M. Yang, *Adv. Funct. Mater.* **2001**, *11*, 95. c) P. Jiang, G. N. Ostojic, R. Narat, D. Mittleman, V. L. Colvin, *Adv. Mater.* **2001**, *13*, 389. d) D. J. Norris, Y. A. Vlasov, *Adv. Mater.* **2001**, *13*, 371.
[3] a) P. Pieranski, *Contemp. Phys.* **1983**, *24*, 25. b) C. C. Striemer, R. Krishnan, P. M. Fauchet, L. Tsybeskov, Q. Xie, *Nano Lett.* **2001**, *1*, 643.
[4] a) S. A. Asher, P. L. Flaugh, G. Washinger, *Spectroscopy* **1986**, *1*, 26. b) N. A. Clark, A. J. Hurd, B. J. Ackerson, *Nature* **1979**, *281*, 57. c) R. J. Carlson, S. A. Asher, *Appl. Spectrosc.* **1984**, *38*, 297. d) C. Reese, S. A. Asher, *J. Colloid Interface Sci.* **2002**, *248*, 41. e) S. A. Asher, *US Patents 4 627 689* and *4 632 517*, **1986**.
[5] a) G. Haacke, H. P. Panzer, L. G. Magliocco, S. A. Asher, *US Patent 5 266 238*, **1993**. b) S. A. Asher, S. Jagannathan, *US Patent 5 281 370*, **1994**. c) S. A. Asher, J. Holtz, L. Liu, Z. Wu, *J. Am. Chem. Soc.* **1994**, *116*, 4997.
[6] a) M. Irie, *Adv. Polym. Sci.* **1993**, *110*, 49. b) Y. Osada, J. Gong, *Prog. Polym. Sci.* **1993**, *18*, 187.
[7] J. M. Weissman, H. B. Sunkara, A. S. Tse, S. A. Asher, *Science* **1996**, *274*, 959.
[8] K. Lee, S. A. Asher, *J. Am. Chem. Soc.* **2000**, *122*, 9534.
[9] J. H. Holtz, S. A. Asher, *Nature* **1997**, *389*, 829.
[10] S. A. Asher, V. L. Alexeev, A. V. Goponenko, A. C. Sharma, I. K. Lednev, C. S. Wilcox, D. N. Finegold, *J. Am. Chem. Soc.* **2003**, *125*, 3322.
[11] J. H. Holtz, J. S. W. Holtz, C. H. Munro, S. A. Asher, *Anal. Chem.* **1998**, *70*, 780.
[12] J. F. Rabek, *Photochemistry and Photophysics*, Vol. 2, CRC Press, Boca Raton, FL **1990**, p. 119.
[13] K. I. Lednev, Y.-Q. Ye, R. E. Hester, J. N. Moore, *J. Phys. Chem.* **1996**, *100*, 13 338.
[14] K. I. Lednev, Y.-Q. Ye, P. Matousek, M. Towrie, P. Foggi, F. V. R. Neuwahl, S. Umapathy, R. E. Hester, J. N. Moore, *Chem. Phys. Lett.* **1998**, *290*, 68.
[15] H. Rau, *Angew. Chem. Int. Ed.* **1973**, *12*, 224.
[16] S. Yamashita, H. Ono, O. Toyama, *Bull. Chem. Soc. Jpn.* **1962**, *35*, 1849.
[17] G. S. Hartley, *Nature* **1937**, *140*, 281.
[18] G. M. Zimmerman, L. Y. Chow, U. J. Paik, *J. Am. Chem. Soc.* **1958**, *80*, 3528.
[19] G. Zimmerman, L. Chow, U. Paik, *J. Chem. Phys.* **1955**, *23*, 825.
[20] J. Griffiths, *Colour and Constitution of Organic Molecules*, Academic Press, New York **1976**.
[21] P. Bortons, S. Monti, *J. Phys. Chem.* **1979**, *83*, 648.
[22] S. Malkin, E. Fisher, *J. Phys. Chem.* **1962**, *66*, 2482.
[23] a) T. Tanaka, L. O. Hocker, G. B. Benedek, *J. Chem. Phys.* **1973**, *69*, 5151. b) T. Tanaka, D. J. Filmore, *J. Chem. Phys.* **1979**, *70*, 1214. c) A. Peters, S. J. Candau, *Macromolecules* **1986**, *19*, 1952. d) A. Peters, S. J. Candau, *Macromolecules* **1988**, *21*, 2278. e) Y. Li, T. Tanaka, *J. Chem. Phys.* **1990**, *92*, 1365. f) M. Annaka, T. Tanaka, *Nature* **1992**, *355*, 430. g) C. J. Durning, K. N. Mormon, Jr., *J. Chem. Phys.* **1993**, *98*, 4275. h) M. Tokita, K. Miyamoto, T. Komai, *J. Chem. Phys.* **2000**, *113*, 1647. i) M.-S. Kang, V. K. Gupta, *J. Phys. Chem. B* **2002**, *106*, 4127.
[24] D. R. Lide, *Handbook of Chemistry and Physics*, 73rd ed., CRC Press, Boca Raton, FL **1992**.
[25] R. Kesavamoorthy, M. S. Super, S. A. Asher, *J. Appl. Phys.* **1992**, *71*, 1116.
[26] S. A. Asher, P. S. Pershan, *J. Phys.* **1979**, *40*, 161.
[27] S. A. Asher, P. S. Pershan, *Biophys. J.* **1979**, *27*, 393.
[28] C. E. Reese, C. D. Guerrero, J. M. Weissman, K. Lee, S. A. Asher, *J. Colloid Interface Sci.* **2000**, *232*, 76.
[29] M. Aslam, A. Dent, *Bioconjugation*, Grove's Dictionaries Inc., New York **1998**.
[30] G. T. Hermanson, *Bioconjugate Techniques*, Academic Press, New York **1996**.

  